RADIO SCIENCE, VOL. 41, RS4006, doi:10.1029/2005RS003367, 2006

A study of the shape of topside electron density profile derived from incoherent scatter radar measurements over Arecibo and Millstone Hill

Xiaoli Luan,[1,2] Libo Liu,[1] Weixing Wan,[1] Jiuhou Lei,[1,3] Shun-Rong Zhang,[4] John M. Holt,[4] and Michael P. Sulzer[5]

Received 5 November 2005; revised 1 March 2006; accepted 3 April 2006; published 19 July 2006.

[1] The shape of the topside electron density (Ne) profile is studied using incoherent scatter radar (ISR) measurements. On the basis of more than 90,000 and 84,000 Ne profiles measured over Arecibo (18.4°N, 66.7°W, dip 49.7°) and Millstone Hill (42.6°N, 71.5°W, dip 71.6°), respectively, shape factors have been derived by fitting the ISR observed profile using a Chapman-type layer with a height-independent scale height. The results reveal that the shape factor shows a general departure from the typically used values of 0.5 (Chapman α layer) except during the night and also undergoes appreciable variation with local time, season, solar activity, and latitude. Over Arecibo, the averaged shape factor is characterized by a daytime maximum of $\sim$0.55–0.75, a nearly constant nighttime value close to 0.5, and a marked morning decline; over Millstone Hill, the shape factor shows pronounced seasonal variations, and the diurnal variation in summer is opposite to that in other seasons. Over both stations, the shape factor exhibits a high correlation with the F_2 layer peak electron density (N_mF_2), and it has strong solar cycle dependence during the late morning hours. It indicates that the temperature structure of the topside ionosphere can explain much of the variation of the shape factor when the plasma density is low, especially during nighttime. During daytime hours, the topside shape factor is thought to be associated with ion-neutral drag during periods of large plasma density.

Citation: Luan, X., L. Liu, W. Wan, J. Lei, S.-R. Zhang, J. M. Holt, and M. P. Sulzer (2006), A study of the shape of topside electron density profile derived from incoherent scatter radar measurements over Arecibo and Millstone Hill, *Radio Sci.*, *41*, RS4006, doi:10.1029/2005RS003367.

1. Introduction

[2] A number of recent studies [*Ezquer et al.*, 1994, 1997; *Huang and Reinisch*, 2001; *Reinisch and Huang*, 2001; *Stankov et al.*, 2003] have estimated the topside electron density (Ne) profile from measurements near the F_2 layer peak, such as the F_2 layer peak height (h_mF_2) or electron density (N_mF_2). It is well known that our knowledge of the topside ionosphere suffers from the lack of observational data, since ground-based ionosondes can probe only up to the F_2 layer peak, and observations from topside sounders and incoherent scatter radar (ISR) are very sparse [*Reinisch and Huang*, 2001]. The simple and analytic Chapman-type layer representation is generally used as a convenient mathematical basis to fit the electron density profiles [*Wright*, 1960; *Fox*, 1994]. Therefore the topside electron density distributions are often represented with a Chapman function using the F_2 layer peak height and density as key parameters. Such fit can be reasonable for the first few hundred kilometers above h_mF_2, and the use of a Chapman-type function to larger heights, like 800 km or more, would require using a scale height that continuously varies with height [*Reinisch*, 2004; *Reinisch et al.*, 2004].

[3] The introduction of a height-dependent scale height into a Chapman α or Chapman β layer can closely match

[1]Institute of Geology and Geophysics, Chinese Academy of Sciences, Beijing, China.
[2]National Satellite Meteorological Center, Chinese Meteorological Administration, Beijing, China.
[3]Now at High Altitude Observatory, National Center for Atmospheric Research, Boulder, Colorado, USA.
[4]Haystack Observatory, Massachusetts Institute of Technology, Westford, Massachusetts, USA.
[5]Arecibo Observatory, National Astronomy and Ionosphere Center, Arecibo, Puerto Rico.

0048-6604/06/2005RS003367$11.00

the observed topside profile [*Fox*, 1994; *Zhang et al.*, 2002; *Lei et al.*, 2004, 2005]. However, a detailed dependence of the topside scale height with height has not yet been developed. Alternatively, a Chapman layer with constant scale height has always been assumed to represent the topside Ne profile. *Ezquer et al.* [1994, 1997] adopted the Chapman layer with scale height equal to atomic oxygen scale height (CHOEA) to predict the ionospheric electron density content (TEC). They found that, given its simplicity, CHOEA is an adequate method to predict TEC at northern low-latitude stations, and it can also predict TEC at the southern crest of the equatorial anomaly with accuracy no worse than various empirical models. *Reinisch and Huang* [2001] introduced a Chapman α layer with a constant scale height derived from measurements of digital ionosonde to represent the topside electron density distribution. This method can also obtain reasonable TEC estimates up to 1000 km [*Huang and Reinisch*, 2001; *Belehaki et al.*, 2003; *Reinisch et al.*, 2004]. On the other hand, *Rishbeth et al.* [1978] proposed a Chapman layer with the neutral scale height of the F_2 layer peak height to estimate the topside electron density content in equivalent winds calculation. This type of the topside TEC estimate has been carried out for nearly three decades [see *Buonsanto et al.*, 1989, 1997; *Luan et al.*, 2004; *Liu et al.*, 2004]. However, the Chapman α layer has a 0.5 factor and the β layer has a 1.0 factor, so the assumption of Chapman α or Chapman β layer with a same constant scale height may lead to significant difference in producing the topside profile [*Stankov et al.*, 2003] and can have much effect on the calculation of the equivalent winds [*Luan et al.*, 2004]. It is reasonable to understand that the Chapman layer with a uniform shape factor and height-independent scale height cannot reproduce the topside Ne profile exactly. Therefore a further investigation on the shape of the topside profile is indeed important.

[4] In the present study, we hope to answer what the shape factors should be in the topside ionosphere if we take the scale height from an atmospheric model as *Ezquer et al.* [1994, 1997] did. The large observational database of incoherent scatter radar (ISR) at two stations, Arecibo (18.4°N, 66.7°W, dip 49.7°) and Millstone Hill (42.6°N, 71.5°W, dip 71.6°) are used to extract the equivalent Chapman shape factors. Next, the local time, seasonal, and solar activity variations of the topside shape factors are analyzed, and their characteristics are interpreted in terms of temperature structure and dynamical processes in the topside ionosphere.

2. Experimental Data and Methodology

[5] The ISR data from Arecibo and Millstone Hill have been retrieved from the Madrigal Database at the Haystack Observatory (http://www.openmadrigal.org). More than 90,000 raw Ne profiles obtained from Arecibo and over 84,000 profiles from Millstone Hill are included in this study. We have used Arecibo ISR experiments from 1966 to 1997, especially those during solar maximum and solar minimum years. These data have a typical altitude resolution of about 23 km prior to 1985 and 37 km in subsequent years. The data over Millstone Hill were selected from 1985 to 2001 when the typical altitude resolution was ~22 km. The median profiles within 15 min at each station are used for our final analysis. Because the ISR observations generally have a time resolution of ~1–3 min over both stations, the number of median profiles used to derive the final results is greatly reduced in comparison with the starting number of raw profiles. Data with a daily mean *Ap* index greater than 30 are not used so as to eliminate the geomagnetic effect. All median profiles are grouped into three seasons (summer, equinox and winter) and two solar flux levels (daily $F_{10.7} < 120$ for solar minimum and $F_{107} \geq 120$ for solar maximum). Each season includes four months: May to August for summer; March, April, September and October for equinox; and November to February for winter. The adopted years of data, the average solar flux, magnetic conditions, and the valid median profile number are listed in Table 1.

[6] First, the peak electron density (N_mF_2) and its height (h_mF_2) are determined by fitting each median Ne profile using a Chapman-type function with a free shape factor and scale height. Then the equivalent shape factor f is obtained from the best match to the topside Ne profile as follows:

$$N_e(h) = N_m\mathrm{F}_2 \exp\{f[1 - z - \exp(-z)]\},$$
$$z = (h - h_m\mathrm{F}_2)/H_m \quad (1)$$

where z represents the reduced height. H_m represents the scale height of neutral atomic O at the peak height, which takes the form kT_n/m_og. T_n is the temperature of atomic O, which is estimated from NRLMSISE00 model [*Picone et al.*, 2002]. Here k is the Boltzmann constant; m_o is the mass of the atomic O.

[7] Our fit is similar to the CHOEA method presented by *Ezquer et al.* [1994, 1997], who use a Chapman α layer ($f = 0.5$) as well as a constant neutral scale height. Hence we refer to our fit as the modified CHOEA method. It should be noted that the use of other scale height values than the model scale height may result in different shape factors. However, in this paper, we focus on what the shape factors should be if we assume a constant neutral scale height. On the other hand, we assume that our calculated scale height is reliable, since the exospheric temperature T_{ex} has been derived from the large ISR databases at Millstone Hill and Arecibo and included in the NRLMSISE00 model [*Picone et al.*, 2002].

Table 1. Details of the ISR Data Used in This Study, Including Mean Solar and Magnetic Activity Levels and the Number of Valid Profiles From Each Site Used in the Analysis

	Solar Maximum	Solar Minimum
	Arecibo	
Years observed	1967–1969, 1981, 1989, 1990–1991	1974–1977, 1985–1987, 1993–1995, 1997
Number of profiles	5640	6262
$\langle Ap \rangle$	11.5	12.5
$\langle F_{10.7} \rangle$	183.5	82.3
	Millstone Hill	
Years observed	1989, 1990–1991, 2000–2001	1985–1987, 1994–1997
Number of profiles	7332	9404
$\langle Ap \rangle$	12.0	10.5
$\langle F_{10.7} \rangle$	189.9	77.7

[8] According to equation (1), the Ne profile can be represented by $\mathrm{Ne}(h) \propto \mathrm{e}^{-fz}$ at a height well above the F_2 layer peak; Therefore the shape factor f can be treated as an equivalent decay coefficient of the electron density with height in the topside ionosphere. Larger values of f result in a quicker decay rate for a constant scale height.

[9] It should be noted that most topside Ne profiles derived from ISR data are reliable up to about 600–800 km. Over Arecibo, observed profiles with a maximum height of ~500 km in 1974–1977 are also included to enrich the database, when these data satisfy certain conditions described below.

[10] For all median profiles, fits are carried out and results are returned for an error or deviation between the fits and data no more than 10%, that is,

$$Err = \left\{ \sum_{n=1}^{N} \left[\left(Ne_{obs.}(n) - Ne_{fit}(n) \right) / Ne_{obs.}(n) \right]^2 \right\} / (N-1) \leq 10\% \quad (2)$$

where N is the number of the observed profile points from the peak height to about 300 km above. In this calculation, data are excluded if the observed profile neither reach the height of ~600 km nor go beyond the height of the half peak density in the topside layer.

3. Analysis and Results

3.1. Samples of Shape Factor

[11] Figure 1 shows two samples of the fit using the modified CHOEA method over each of the stations. The results are compared with the observed Ne profile and the estimated profiles using the IRI2000 model [*Bilitza*, 2001]. The IRI2000 model prediction has incorporated the observed N_mF_2 and h_mF_2 as input parameters. These samples represent a smaller shape factor of 0.35 and a larger one of 0.71, respectively. As can be seen, the modified CHOEA method generally matches the observations well up to ~300–400 km above the F_2 layer

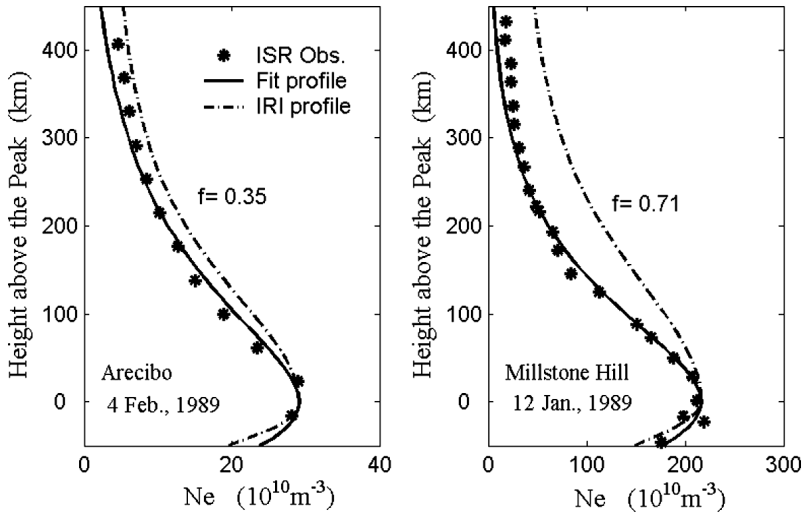

Figure 1. Examples of the fit (solid curve) to the observed topside profile (asterisks) by the Chapman-type function using the equivalent shape factor f. Data (left) at Arecibo (~0530 LT) and (right) at Millstone Hill (~1230 LT) are shown. A comparison with output from the IRI2000 model (dash-dotted curve) is also presented.

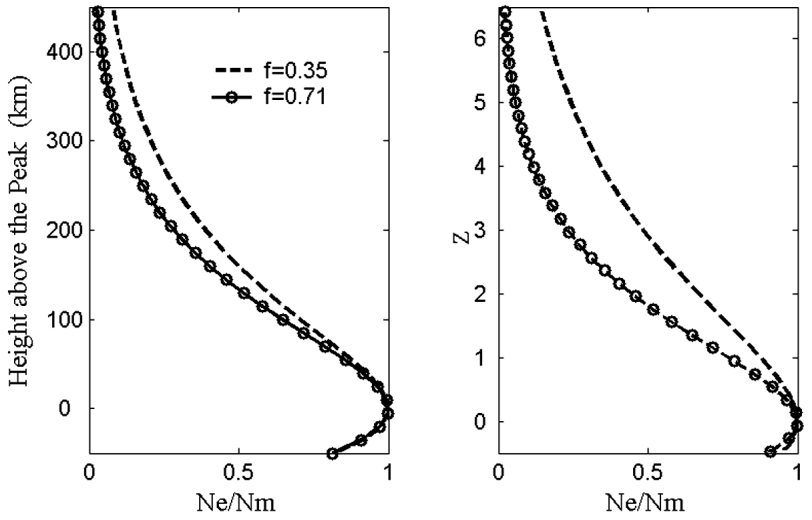

Figure 2. Ne profile shape in the topside F region corresponding to the two factors (0.35 and 0.71) in Figure 1: (left) dependence of the Ne profile shape on the height above the F_2 layer peak and (right) its dependence on the reduced height $z = (h - h_mF_2)/H_m$.

peak height, h_mF_2. Fortunately, the neutral scale height H_m is around 40–50 km at solar minimum and 60–80 km at solar maximum over the two stations (not presented here). The fit above that height tends to underestimate the electron density, but seems to have little effect on the ionospheric TEC estimation, because the electron density declines markedly. The IRI prediction appears to overestimate the electron density, especially over Millstone Hill. Figure 2 shows the corresponding variations of the two Ne profiles with height and the reduced height. For the smaller shape factor, the Ne exhibits much slower decay with both the actual and the reduced height.

[12] Figure 3 shows all the samples of the equivalent shape factors over Arecibo and Millstone Hill. Over Arecibo, the average of all shape factors approximates the Chapman α distribution ($f = 0.5$) at night, but exceeds 0.5 during daytime. Over Millstone the average is closer to 0.5 except during the predawn hours. The shape factors are more variable over Millstone Hill than those over Arecibo, presumably because there are more distinct seasonal variations of the shape factors over Millstone Hill (see Figures 4 and 5).

3.2. Diurnal and Seasonal Variations

[13] The equivalent shape factors are binned according to season and solar activity over both stations. As shown in Figure 4, over Arecibo the average shape factors show a marked diurnal variation for all seasons and solar activity levels. They are characterized by a daytime maximum, a nearly constant value at night, and large morning decline. The daytime maximum values are between 0.55 and 0.75 and the morning minima are between 0.35 and 0.45. The shape factors build up the larger daytime peak in winter at solar maximum and the smaller morning value in winter at solar minimum. The daytime maximum of the shape factors occurs in the afternoon (~1400–1600 LT) in summer, whereas it peaks before midday (~0900–1100 LT) in winter. During equinox, the shape factors have an afternoon peak at solar minimum while they are nearly constant during daytime at solar maximum. The larger shape factors by day may be attributed to the significant influence of the daylight photochemical processes as a source of the electron density production at lower altitudes.

[14] The morning decline is a prevalent feature in each season over Arecibo. At solar minimum, the shape factors exhibit a marked decline starting in the early morning hours, with a predawn end in equinox and winter. However, a similar decline starts about three hours later in summer with an end after sunrise. The features are similar at solar maximum, while the decline starts and ends about one hour earlier. From evening to early morning hours (~2000–0200 LT), the shape factors maintain a constant value close to 0.5. The diurnal variations of the shape factors generally have two patterns. In winter at both solar activity levels and during the equinox at solar maximum, the shape factors generally increase quickly from a morning minimum to a maximum before midday, decreasing slowly to a nearly constant evening value, whereas in summer at both solar activity levels and during the equinox at solar minimum,

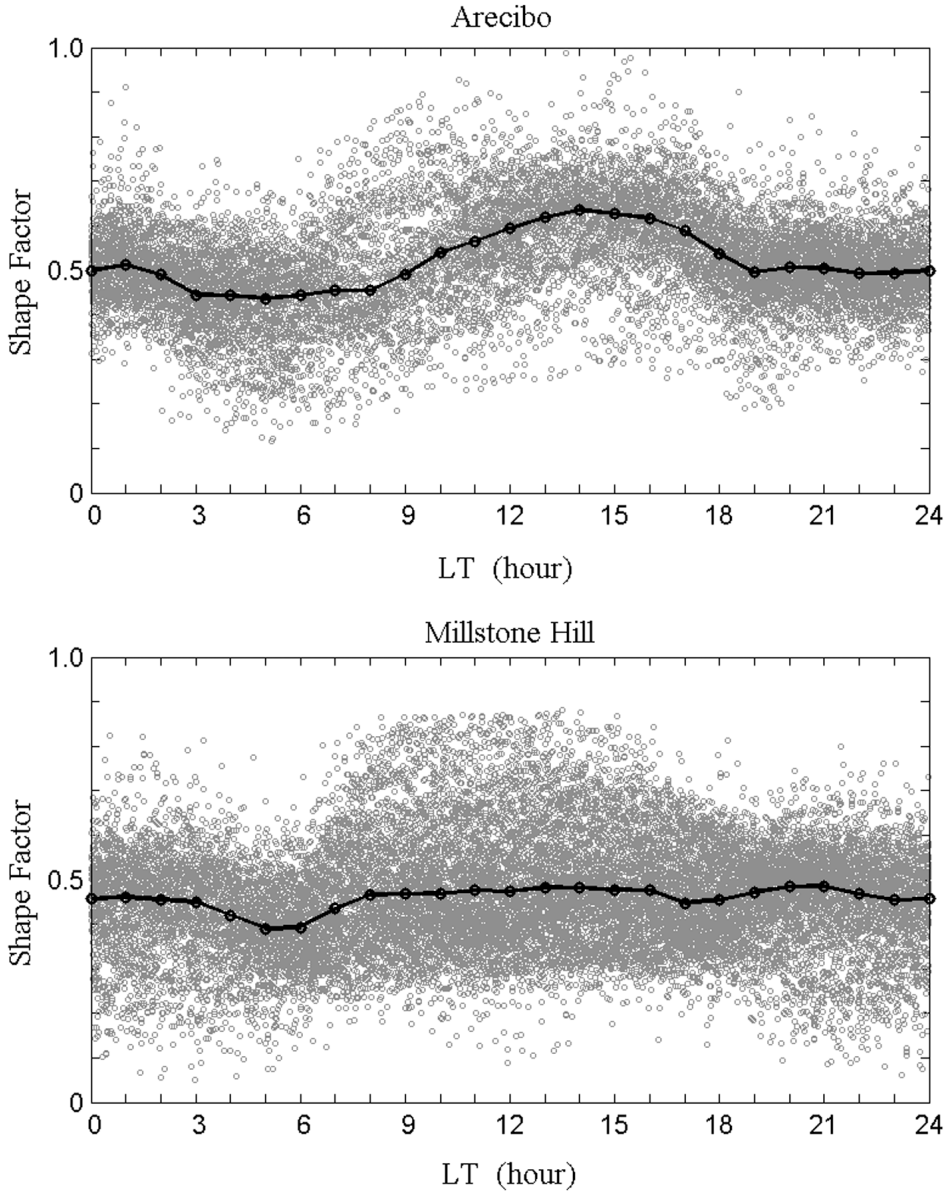

Figure 3. Plot containing all of the derived shape factors from (top) Arecibo and (bottom) Millstone Hill data sets. The median value is indicated by the solid curve with circles.

they slowly increase from the morning minimum until an afternoon peak is formed and then decreased quickly to an evening value. Moreover, the shape factors show a small sunset fluctuation during most seasons and levels of solar activity.

[15] As seen in Figure 5, over Millstone Hill, the average shape factors do not show sharp peaks during the day under most conditions, but they have distinct seasonal and solar activity variations. They are generally larger during the day than at night in fall and winter, similar to those over Arecibo, while in summer the diurnal trend is opposite to the Arecibo case. The daytime shape factors are lower in summer and higher in winter at both solar minimum and maximum. During daytime, the averaged shape factors are only about 0.35 in summer at solar minimum, while they can reach

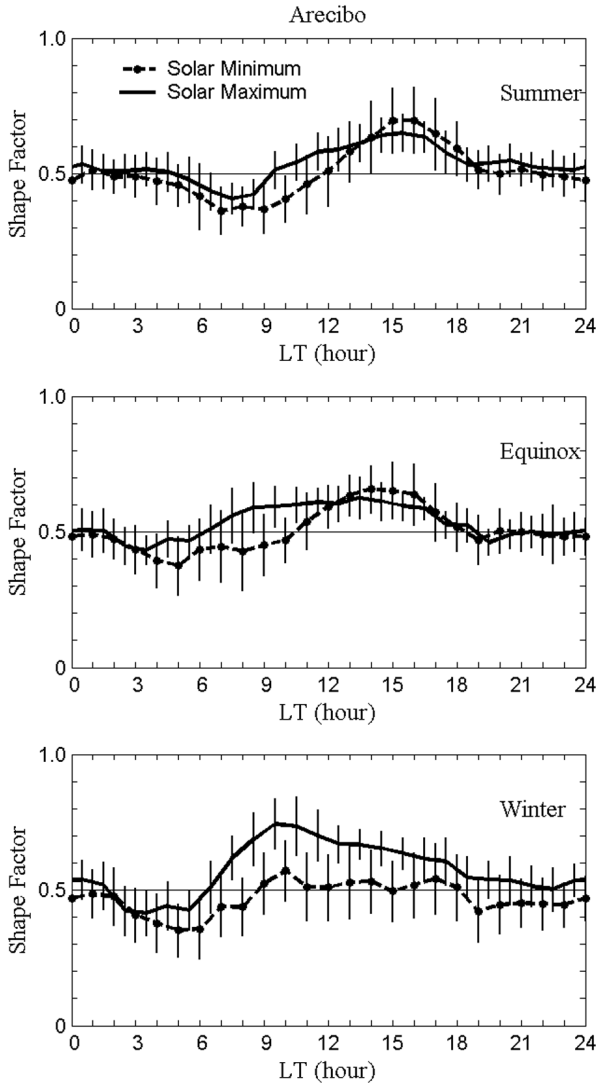

Figure 4. Averaged seasonal shape factor during solar maximum and minimum derived from Arecibo ISR measurements of the topside ionosphere. The hourly standard deviation is also denoted.

values near 0.75 in winter at solar maximum. During night, the shape factors are between 0.29 and 0.4 in winter at solar minimum, much lower than those in the other groups. A gradual morning decline is generally presented in all seasons, followed by rapid increase during winter and equinox, while it does not recover until the evening hours in summer.

[16] At both stations, the shape factors are generally larger at solar maximum than solar minimum (Figures 4 and 5). Their solar cycle dependence is strong from near sunrise to midday over Arecibo. Over Millstone Hill, strong solar cycle dependence persists from sunrise to the late afternoon, and even into the early morning hours during winter. Over both stations, the larger difference of the shape factors between solar minimum and solar maximum occurs near midday in winter, with a difference of 0.2–0.25.

3.3. The f-N_mF_2 Correlation

[17] In summer over Millstone Hill, the largest shape factors occur during the evening hours (2000–2100 LT), similar to the F_2 layer peak density, which is a marked feature of the evening enhancement [*Holt et al.*, 2002]. Over both stations, we found that the peak of the shape

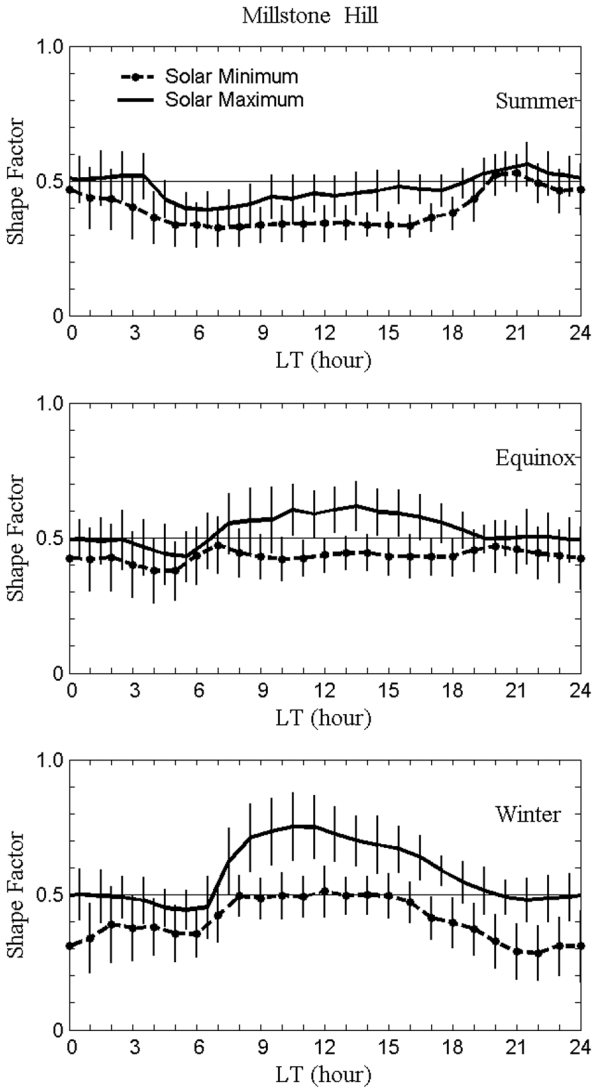

Figure 5. Same as Figure 4 but for Millstone Hill.

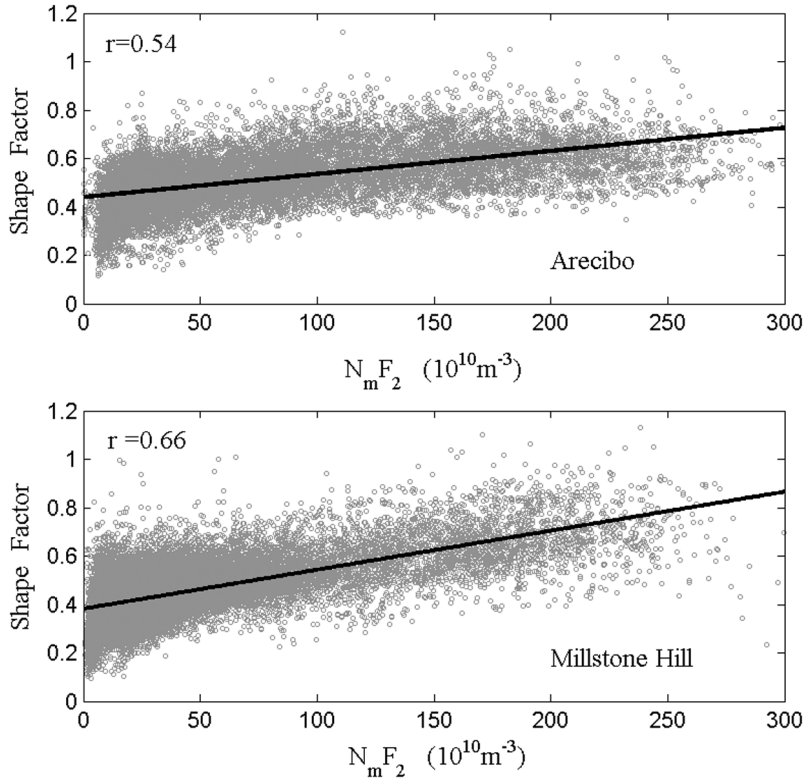

Figure 6. Correlation between the shape factors and the peak electron density (N_mF_2) derived from (top) Arecibo and (bottom) Millstone Hill measurements. The correlation coefficient is denoted by r, and the solid curve shows the least squares fit to the data.

factors tends to occur when N_mF_2 attains its diurnal maximum. Figure 6 presents the correlation between the shape factors and the F_2 layer peak electron density (N_mF_2). It shows correlation coefficients of 0.54 and 0.66 over Arecibo and Millstone Hill, respectively. The close relationship between the shape factors and N_mF_2 may be attributed to a common mechanism, such as photochemical processes, variation of the ion and electron temperature, or background neutral winds.

4. Discussion

[18] The electron density distribution is assumed to take the form $\mathrm{Ne}(h) \propto e^{-z/2}$ well above the F_2 layer peak, suggesting a shape factor value of 0.5, if the ionosphere is in the condition of diffusive equilibrium [*Rishbeth and Garriott*, 1969]. Our results show that the theoretical shape factor ($f = 0.5$) is generally close to the averaged value at night over both stations. However, much lower shape factors (<0.5) occur during the morning decrease over both stations, as well as during the winter night at solar minimum over Millstone Hill (see Figures 4 and 5). A considerable departure from 0.5 appears during daytime hours when the equivalent shape factors are in the vicinity of their maximum in each season over Arecibo. Over Millstone Hill, a much larger daytime departure from 0.5 occurs in summer at solar minimum (<0.5) and in winter at solar maximum (>0.5).

[19] To a certain extent, the shape factor f is similar to the equivalent slab thickness as an indicator of the topside electron density content. The equivalent slab thickness (τ) is defined as the breadth (in kilometers) of the ionosphere of uniform electron density equal to the peak density N_mF_2, that is, the ratio of the total electron density content (TEC) to N_mF_2, $\tau = \mathrm{TEC}/N_mF_2$. Lower f values correspond to a slower decay of the electron density with height, suggesting a greater topside equivalent slab thickness. By enhancing the topside contribution to the TEC, the morning decline of f may coincide with the predawn increase of the equivalent slab thickness. It is interesting that the morning decline of f is generally more distinct over Arecibo than over Millstone

Hill, especially in winter, and the appearance of a predawn maximum of the slab thickness is also more pronounced in lower latitudes [*Davies and Liu*, 1991].

[20] The dynamics in the topside ionosphere are dominated by plasma diffusion, in which the topside temperature structure, the ion composition and concentration, and ion-neutral coupling are the controlling factors. In the present study, the shape factors represent the shape from around the F_2 layer peak extending upward several hundreds of kilometers to heights where the charge exchange and photochemical effects are small. Therefore the variation of the topside shape factors can be understood in the context of temperature structure and dynamical effects. According to *Lockwood and Titheridge* [1982], the field-aligned diffusion velocity ($W_{d//}$) can be expressed as

$$W_{d//} = V_{i//} - U_{//} = -\frac{\sin I}{m_i \nu_{in}} \left\{ \frac{1}{N_i} \frac{d}{dh} [N_i k (T_i + T_e)] + m_i g \right\} \quad (3)$$

where $W_{d//}$, $V_{i//}$ and $U_{//}$ are field-aligned diffusion velocity, velocity of ion and neutral components, respectively. I is the magnetic inclination. m_i and N_i are the ion mass and density. k is the Boltzmann constant. T_e and T_i are the electron and ion temperature, respectively; ν_{in} is ion-neutral collision frequency; and g is the acceleration of gravity.

[21] Well above the F_2 layer peak, the shape factors relate to the electron density in the form of $dN_i/dh = -fN_i(1 - e^{-z})/H_m \approx -fN_i/H_m$ on the basis of equation (1). Hence if the vertical diffusion velocity ($W_d = W_{d//}\sin I$) is considered, then the shape factors can be estimated from equation (3) as follows:

$$f = \frac{0.5}{1 + \Delta T/T_n} \frac{m_i}{m_o} \left(1 + C_1 \frac{dT_r}{dh} + C_2 W_d \right) \quad (4)$$

where $T_r = (T_i + T_e)/2$ is mean plasma temperature, $\Delta T = T_r - T_n$ is the difference between plasma and neutral temperature, m_i and m_o are the mean ion mass and mass of the atomic O. W_d is the upward diffusive velocity, and the two coefficients C_1 and C_2 are expressed as $C_1 = k/(2m_i g)$ and $C_2 = \nu_{in}/(g\sin^2 I)$.

[22] The coefficient C_2 denotes that the effect of plasma diffusion is constrained by the ion-neutral collision frequency in the topside ionosphere. The ratio of mean ion mass to the neutral atomic O, m_i/m_o, represents the effect of the O^+–H^+ transition height. In the present study the shape factors are mostly derived below the O^+–H^+ transition height [*Kutiev et al.*, 1980], such that the ratio can be estimated to the value of 1, corresponding to a condition of O^+ ion dominance.

[23] According to equation (4), it seems that the topside temperature structure, and the ion-neutral drag due to plasma diffusion, can be largely responsible for the variation of the shape factors when diffusion processes dominate. The relative importance of these effects is assessed over Millstone Hill with the help of an empirical model [*Holt et al.*, 2002] for ion and electron density, temperature, and ion velocity, and the HWM93 model [*Hedin et al.*, 1996] for neutral winds, and the NRLMSISE00 model for neutral temperature.

[24] Figure 7 shows a comparison of the observed shape factors with the estimates from equation (4) for different conditions over Millstone Hill. The estimated shape factors are calculated assuming two conditions: (1) considering the effect of diffusive velocity ($W_d \neq 0$) and (2) assuming diffusive equilibrium ($W_d = 0$). The results show that, the two estimated results and the observed shape factors are similar from around sunset to sunrise, and that the $W_d = 0$ results are consistent with observations all day during summer. During daytime, the $W_d \neq 0$ results can provide a much closer estimate to the observation during winter and equinox regardless of solar activity. This may be explained by the contribution of ion-neutral drag, which is significant when the plasma density is enhanced, or when the ion-neutral collision rate is large. Over Millstone Hill, the plasma density in winter is enhanced during daytime when the midday electron density maximum (winter anomaly) occurs, and it peaks during the evening hours in summer. Therefore we can infer that the topside temperature structure can influence the topside Ne shape under conditions of lower electron density, during which the ion-neutral coupling is weak. Otherwise, the shape of the topside ionosphere can be greatly influenced by the effects of ion-neutral drag.

[25] If the above inference is true, then the morning decline feature and the much smaller shape factors at other times can be associated with features of the electron temperature T_e, such as the T_e predawn enhancement or the nighttime enhancement of T_e in winter [*Evans*, 1973; *Zhang and Holt*, 2004; *Sharma et al.*, 2005]. Over Millstone Hill, T_e in the height of ~500 km can increase by two or three times in the early morning, while the growth of T_i is not obvious [*Zhang and Holt*, 2004]. The effects of plasma diffusion and plasma temperature gradients may provide additional contributions. The height dependence of the sunrise effect on N_e may also have some effect. Similarly, the shape factors with much smaller daytime values in summer may also be attributed to a large and nearly constant T_e [*Zhang and Holt*, 2004] under the condition of insignificant or low values of ion-neutral drag. A weak sunset fluctuation in the shape factors is generally present over Arecibo while absent over Millstone Hill. It may be caused by the secondary enhancement of electron and ion temperatures at low latitudes, which has been observed by the SROSS-C2 satellite over the Indian region between 5°N and 35°N [*Sharma et al.*, 2005].

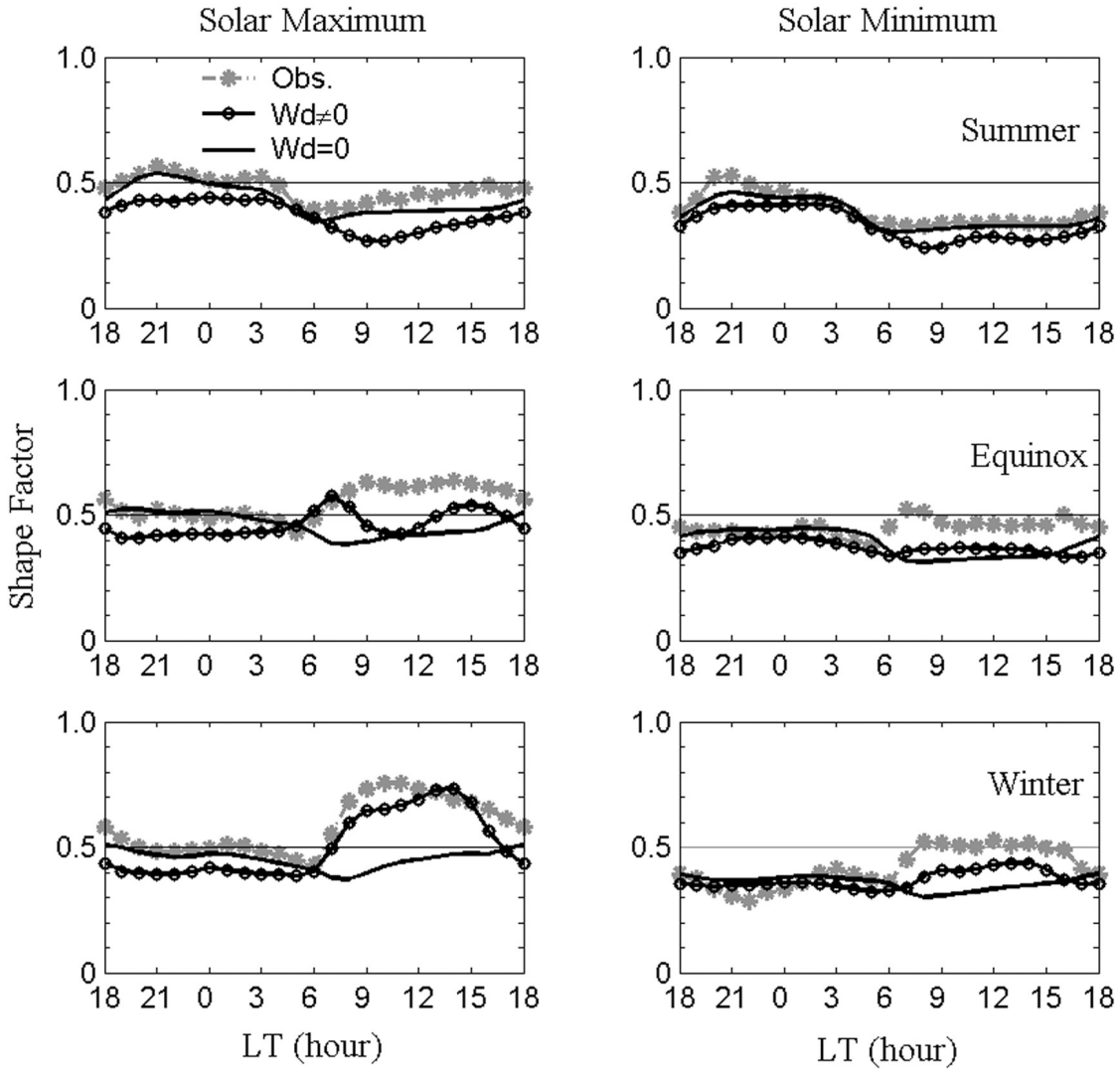

Figure 7. Observed shape factors (dash-dotted curve with asterisks) compared with estimated values derived from empirical models for Millstone Hill (see equation (4) in the text). The solid curve assumes diffusive equilibrium ($W_d = 0$), whereas the solid curve with circles shows the effect of taking plasma diffusion ($W_d \neq 0$) into account.

[26] The movement of the ionosphere due to neutral winds may be a primary cause of the variations of topside temperature and plasma density, and consequently the shape of the topside ionosphere is modified. The effect of the ion composition; that is, the O^+–H^+ transition height are neglected in this analysis. A departure from the O^+ ion dominating condition can lead to smaller shape factor due to a decrease of mean ion mass, as seen from equation (4), which can most likely occur during night when the transition height is low. It may explain the difference between the observed and the estimated shapes during ~2100–2300 LT in winter and at solar minimum over Millstone Hill (Figure 7).

[27] The observed shape factors in this analysis represent mean shape of the topside *F* region. They can be expected to be smaller at higher altitude, because of the relatively larger temperature difference between the plasma and neutral components, and a smaller effect due to ion-neutral drag (equation (4)). If the thermal equilibrium condition ($T_e = T_i = T_n$) is met, the shape factors will be very close to 0.5 during night when the temperature gradient and plasma density is small. This may explain the general approximation of the topside

shape to the Chapman α layer during most nighttime hours over both stations, when ion-neutral drag and the difference between the plasma and the neutral components is insignificant.

5. Conclusions

[28] We have derived the equivalent shape factor of a Chapman-type layer with a neutral scale height by fitting the observed ISR Ne profiles over the Arecibo and Millstone Hill Observations. The Chapman α layer has a 0.5 factor and the β layer has a 1.0 factor. Our results show that the shape factors vary with local time, season, solar activity and latitude; furthermore, they exhibit a general departure from the widely used value of 0.5 except during nighttime.

[29] Over Arecibo, the averaged shape factors are characterized by a daytime maximum of $\sim$0.55–0.75, a nearly constant nighttime value close to 0.5, and a deep morning minimum of $\sim$0.35–0.45. A large daytime peak of about 0.75 occurs in winter at solar maximum and a minimum morning value of about 0.35 is prevalent in winter during solar minimum. Over Millstone Hill, the diurnal variation of the averaged shape factors shows tendencies of a daytime and nighttime plateau, and a slow morning decline. The averaged shape factors also reveal pronounced seasonal variations. They are larger by day than at night in fall and winter, but the reverse seems to be the case during summer. The shape factors are much smaller than 0.5 during daytime hours in summer at solar minimum. Shape factors as low as $\sim$0.30 are also found in the winter evening ($\sim$2200 LT) during solar minimum.

[30] Note that over both stations, the shape factors exhibit a positive correlation with the F_2 layer peak density (N_mF_2) and have strong solar cycle dependence during the late morning hours prior to midday. Also over both stations, there are evident features of the morning decline in each season and the marked late morning peak ($\sim$0900–1100 LT) appears in winter and at solar maximum. This would suggest that the morning decline may be due to the well-known phenomenon of the predawn enhancement in electron temperature. The study also suggests that the shape factors are associated with the ion-neutral drag effect, when the plasma density is relatively large. Our results may shed some light on the estimation of the topside electron density content at locations where direct observations are not feasible.

[31] **Acknowledgments.** This research was supported by the KIP Pilot Project (kzcx3-sw-144) of the Chinese Academy of Sciences, National Natural Science Foundation of China (40574071), and National Important Basic Research Project (G2000078407). We thank the members of the Haystack Observatory Atmospheric Sciences Group for assembling and maintaining the Madrigal database containing the Millstone Hill and Arecibo incoherent scatter radar observations. The Millstone Hill incoherent scatter radar is supported by a cooperative agreement between the U.S. National Science Foundation and the Massachusetts Institute of Technology. The Arecibo Observatory is the principal facility of the U.S. National Astronomy and Ionosphere Center, which is operated by Cornell University under a cooperative agreement with the National Science Foundation.

References

Belehaki, A., N. Jakowski, and B. W. Reinisch (2003), Comparison of ionospheric ionization measurements over Athens using ground ionosonde and GPS-derived TEC values, *Radio Sci.*, *38*(6), 1105, doi:10.1029/2003RS002868.

Bilitza, D. (2001), International reference ionosphere 2000, *Radio Sci.*, *36*, 261–275.

Buonsanto, M. J., J. E. Salah, K. L. Miller, W. L. Oliver, R. G. Burnside, and P. G. Richards (1989), Observations of neutral circulation at mid-latitudes during the equinox transition study, *J. Geophys. Res.*, *94*, 16,987–16,997.

Buonsanto, M. J., M. J. Starks, J. E. Titheridge, P. G. Richards, and K. L. Miller (1997), Comparison of techniques for derivation of neutral meridional winds from ionospheric data, *J. Geophys. Res.*, *102*, 14,477–14,484.

Davies, K., and X. M. Liu (1991), Ionospheric slab thickness in middle and low latitudes, *Radio Sci.*, *26*, 997–1005.

Evans, J. V. (1973), Seasonal and sunspot cycle variation of *F* region electron temperatures and protonospheric heat flux, *J. Geophys. Res.*, *78*, 2344–2349.

Ezquer, R. G., N. Ortiz de Adler, and T. Heredia (1994), Predicted and measured total electron content at both peaks of the equatorial anomaly, *Radio Sci.*, *29*, 831–838.

Ezquer, R. G., N. Jakowski, and C. A. Jadur (1997), Predicted and measured total electron content over Havana, *J. Atmos. Terr. Phys.*, *59*, 591–596.

Fox, M. W. (1994), A simple, convenient formalism for electron density profiles, *Radio Sci.*, *29*, 1473–1491.

Hedin, A. E., et al. (1996), Empirical wind model for the upper, middle and lower atmosphere, *J. Atmos. Terr. Phys.*, *58*, 1421–1447.

Holt, J. M., S. Zhang, and M. J. Buonsanto (2002), Regional and local ionospheric models based on Millstone Hill incoherent scatter radar data, *Geophys. Res. Lett.*, *29*(8), 1207, doi:10.1029/2002GL014678.

Huang, X., and B. W. Reinisch (2001), Vertical electron content from ionograms in real time, *Radio Sci.*, *36*, 335–342.

Kutiev, I., R. A. Heelis, and S. Aanatani (1980), The behavior of the O^+-H^+ transition level at solar maximum, *J. Geophys. Res.*, *85*, 2366–2372.

Lei, J., L. Liu, W. Wan, S. Zhang, and J. M. Holt (2004), A statistical study of ionospheric profile parameters derived from Millstone Hill incoherent scatter radar measurements, *Geophys. Res. Lett.*, *31*, L14804, doi:10.1029/2004GL020578.

Lei, J., L. Liu, W. Wan, and S. Zhang (2005), Variations of electron density based on long-term incoherent scatter radar and ionosonde measurements over Millstone Hill, *Radio Sci.*, *40*, RS2008, doi:10.1029/2004RS003106.

Liu, L., X. Luan, W. Wan, J. Lei, and B. Ning (2004), Solar activity variations of equivalent winds derived from global ionosonde data, *J. Geophys. Res.*, *109*, A12305, doi:10.1029/2004JA010574.

Lockwood, M., and J. E. Titheridge (1982), Departures from diffusive equilibrium in the topside *F*-layer from satellite sounding, *J. Atmos. Terr. Phys.*, *44*, 425–440.

Luan, X., L. Liu, W. Wan, J. Lei, and T. Yu (2004), Climatology of the *F*-layer equivalent winds derived from ionosonde measurements over two decades along the 120°–150°E sector, *Ann. Geophys.*, *22*, 2785–2796.

Picone, J. M., A. E. Hedin, D. P. Drob, and A. C. Aikin (2002), NRLMSISE-00 empirical model of the atmosphere: Statistical comparisons and scientific issues, *J. Geophys. Res.*, *107*(A12), 1468, doi:10.1029/2002JA009430.

Reinisch, B. W. (2004), Tenth International Digisonde Training Seminar at UMass Lowell Reviews State of Real Time Mapping of the Ionosphere, *IEEE Antennas Propag. Mag.*, *45*, 110–117.

Reinisch, B. W., and X. Huang (2001), Deducing topside profiles and total electron content from bottomside ionograms, *Adv. Space Res.*, *27*, 23–30.

Reinisch, B. W., X. Huang, A. Belehaki, and R. Ilma (2004), Using scale heights derived from bottomside ionograms for modeling the IRI topside profile, *Adv. Radio Sci.*, *2*, 293–297.

Rishbeth, H., and O. K. Garriott (1969), *Introduction to Ionospheric Physics*, Elsevier, New York.

Rishbeth, H., S. Ganguly, and J. C. G. Walker (1978), Field-aligned and field-perpendicular velocities in the ionospheric F_2 layer, *J. Atmos. Terr. Phys.*, *40*, 767–784.

Sharma, D. K., J. Rai, M. Israil, and P. Subrahmanyam (2005), Diurnal, seasonal and latitudinal variations of ionospheric temperatures of the topside F region over the Indian region during solar minimum (1995–1996), *J. Atmos. Sol. Terr. Phys.*, *67*, 269–274.

Stankov, S. M., N. Jakowski, S. Heise, P. Muhtarov, I. Kutiev, and R. Warnant (2003), A new method for reconstruction of the vertical electron density distribution in the upper ionosphere and plasmasphere, *J. Geophys. Res.*, *108*(A5), 1164, doi:10.1029/2002JA009570.

Wright, J. V. (1960), A model of the *F* region above h_mF_2, *J. Geophys. Res.*, *65*, 185–191.

Zhang, M. L., S. M. Radicella, I. Kersley, and S. A. Pulincts (2002), Results of the modeling of the topside electron density profile using the Chapman and Epstein function, *Adv. Space Res.*, *29*, 871–876.

Zhang, S.-R., and J. M. Holt (2004), Ionospheric plasma temperatures during 1976–2001 over Millstone Hill, *Adv. Space Res.*, *33*, 963–969.

J. M. Holt and S.-R. Zhang, Haystack Observatory, Massachusetts Institute of Technology, Westford, MA 01886, USA.

J. Lei, High Altitude Observatory, National Center for Atmospheric Research, Boulder, CO 80307, USA. (leijh@ucar.edu)

L. Liu and W. Wan, Institute of Geology and Geophysics, Chinese Academy of Sciences, Beijing 100029, China. (liul@mail.igcas.ac.cn; wanw@mail.igcas.ac.cn)

X. Luan, National Satellite Meteorological Center, Chinese Meteorological Administration, Beijing 100081, China. (luanxl@nsmc.cma.gov.cn)

M. P. Sulzer, Arecibo Observatory, National Astronomy and Ionosphere Center, HC3 Box 53995, Arecibo, Puerto Rico 00612.